Title: Transcranial direct current stimulation of the supplementary motor area modulates behavioral and peripheral electrophysiological measures of motor preparation

Running title: SMA stimulation and motor preparation

Authors

Ashutosh Kumar[1] **https://orcid.org/0009-0003-6766-9382**
Aditya Murthy[12] https://orcid.org/0000-0001-7155-8616

Affiliations

1. Movement Control Lab, Centre for Neuroscience, Indian Institute of Science, Bengaluru 560012, India.
2. Corresponding author

Corresponding author

Aditya Murthy, PhD
Movement Control Lab, Centre for Neuroscience, Indian Institute of Science
CV Raman Road, Bengaluru 560012, India
Email: **adi@iisc.ac.in**
ORCID: https://orcid.org/0000-0001-7155-8616

Author contributions (Credits)

Ashutosh Kumar - Conceptualization, Methodology, Investigation, Formal Analysis, Data Curation, Writing – Original Draft, Writing – Review & Editing, Visualization

Aditya Murthy - Conceptualization, Methodology, Writing – Review & Editing, Supervision, Project Administration

Conflicts of interest

The authors declare no competing interests.

Data and code availability

data and analysis code will be made available upon reasonable request to the corresponding author, in accordance with institutional and ethical requirements.

Ethics approval

Human research was approved by the Institutional Human Ethics Committee, Indian Institute of Science, Bengaluru **(No - 01/23.02.2023)**

Acknowledgments

We thank all study volunteers for their time and patience during the experiments. We are grateful to Kalpajyoti Hazarika for technical assistance and to Ankita Das for her help with subject preparation and data collection.

Funding

This work was supported by a grant from the Science and Engineering Research Board/Anusandhan National Research Foundation (SERB/ANRF), Government of India, and additional intramural funding from the Indian Institute of Science (IISc).

Abstract

Converging evidence has shown that the Supplementary Motor Area (SMA) is involved in the preparation of movements. Such preparatory activity has been traditionally thought to lead to shorter reaction times by allowing the motor network to settle into states favourable to motor execution without directly engaging the peripheral musculature, limiting such preparatory states to central neural processes only. We revisited this issue by recording motor unit related activity using high-density surface EMG grid electrodes, from the Anterior Deltoid muscle, a proximal muscle, during a delayed reach task. We observed that anodal stimulation of the supplementary motor area (SMA) enhances motor preparation by shortening reaction times, while simultaneously enhancing motor unit activity. Additionally, we found that the SMA stimulation also produced a subsequent increase in movement velocities due to the increase activation of larger amplitude motor units. Taken together, we suggest that motor preparatory states involve an active interaction between central and peripheral processes with direct descending SMA outputs to the spinal cord providing a link between cortical preparation and muscle readiness, resulting in decreased reaction times. In addition, the increased gain of such central to peripheral interactions also increases the subsequent gain during the execution phase via modulating larger amplitude motor unit activation, resulting in increased response vigour.

Keywords: low threshold motor units; anodal stimulation; reaction time; high-density EMG; hold time effect; delay period

Introduction

The execution of skilled voluntary movements relies on motor preparation, which involves organising the motor network into states that favour subsequent movement execution (Shenoy et al., 2013; Churchland et al., 2006,2010,2012; Kaufman et al., 2014; Elsayed et al., 2016). Studies have also shown that the Supplementary Motor Area (SMA) is a key node in the network that orchestrates this preparatory process (Tanji, 1994; Picard & Strick, 1996; Nachev et al., 2008), with convergent human evidence from MRI and ERP/EEG demonstrating SMA/pre-SMA engagement during readiness and initiation (Tanji,1984; Cunnington et al., 2002; Jenkins et al., 2000; Shibasaki & Hallett, 2006; Lau et al., 2006). For example, electrophysiological studies in non-human primates show that neurons in medial premotor cortex (SMA/pre-SMA) exhibit robust delay-period activity that ramps during preparation and anticipates movement onset, and ceases firing just prior to execution, distinguishing preparatory and execution phases (Tanji & Shima, 1994; Tanji, 1994; Crammond & Kalaska, 2000; Tanji & Kurata, 1982,1985; Shima & Tanji, 2000; Tanji, 2001). This temporal signature positions the SMA as a critical hub for establishing a “preparatory motor set” — a state of enhanced motor readiness marked by gradual buildup of cortical activity that preconfigures the motor system for rapid initiation of voluntary movements (Tanji, 1994; Nachev et al., 2008; Picard & Strick, 1996; Churchland et al., 2012; Shenoy et al., 2013, Carlson et al., 2015). Human EEG studies further confirm this role, identifying slow-rising movement-related potentials over medial frontal cortex/SMA that begin well before movement execution, including the classic Bereitschaftspotential and its early and late components (Shibasaki & Hallett, 2006; Deecke & Kornhuber, 1978; Cunnington et al., 2002; Colebatch, 2007).

The behavioral relevance of preparatory activity is evident in reaction time paradigms, where introducing a delay period between target appearance and go cue consistently results in faster response times - the "hold time effect" (Churchland et al., 2006,2010; Shenoy et al., 2013; Lara et al., 2018). Manipulations of the hold time effect by transcranial direct current stimulation (tDCS) over the SMA have also been used to establish causal relationships between SMA activity and motor preparation in human subjects. Studies applying anodal tDCS over the SMA have demonstrated polarity-dependent effects on reaction time performance, consistent with modulating preparatory activation levels toward an action threshold (Carlsen et al., 2015; Sadler et al., 2022; Sato et al., 2024).

Despite the presence of the hold time effect, traditional EMG methods have largely failed to detect muscle activity during preparatory periods (Tanji & Evarts, 1976; Kaufmann et al., 2014), leading to the notion that preparatory states are confined to central neural processes. However, early work by Mellah et al. (1990) showed changes in motor unit excitability during movement preparation in non-human primates, suggesting that preparatory processes might reach the peripheral musculature. In addition, recent work by Rungta and Murthy (2023) used high-density surface EMG to show that early motor preparation can be detected peripherally through context-specific recruitment of small-amplitude motor units during the delay period in reaching tasks in humans. These "ramping" motor units displayed spatially specific activity patterns that correlated with reaction times, providing direct evidence of preparatory neural drive extending to peripheral neuromuscular readiness.

The presence of peripheral preparatory signatures raises a crucial question: do cortical neuromodulation effects, such as those induced by SMA tDCS, translate to measurable changes in the early recruitment patterns of these preparatory motor units? The present study addresses this question by investigating whether anodal tDCS applied to the SMA modulates the early preparatory activity of low-threshold motor units in the anterior deltoid muscle during a randomized delayed reach task. By combining targeted cortical stimulation with high-density EMG recordings, we aimed to establish a direct link between cortical neuromodulation and peripheral manifestations of motor preparation.

Materials and Methods

Participants

Twenty healthy, right-handed volunteers (age range: 19–26 years) participated in the experiment. All reported normal or corrected to normal vision, no history of neurological or psychiatric disorders, and no use of medication affecting the central nervous system. Written informed consent was obtained from all participants in accordance with the approved protocol of the Institutional Human Ethics Committee, Indian Institute of Science, Bengaluru. Participants received monetary compensation for their time. we initially recruited 12 participants in the anodal tDCS condition (anode over the supplementary motor area (SMA)); however, only 9 participants remained for further analysis because they demonstrated a clear hold-time effect, which was necessary to address the present research question. The control

group was formed by combining participants from the sham and reverse polarity conditions. Initially, 5 participants underwent sham stimulation (identical electrode placement without sustained actual current), and 3 participants underwent reverse-polarity stimulation (electrodes swapped to produce anterior to posterior current flow). Because the reverse polarity group showed behavioral outcomes qualitatively similar to the sham group, their data were pooled to yield a combined control sample of eight participants. One participant from this combined cohort was subsequently excluded due to extremely poor task performance (correct responses in only 20 out of 100 trials across all conditions), resulting in a final control group size of seven.

Experiment Setup

Stimulus presentation and data collection were conducted using NIMH MonkeyLogic (Hwang et al., 2019) in MATLAB (MathWorks Inc.). Visual stimuli appeared on a 21.5-inch XP Pen Artist Display 22R Pro tablet (Hanvon Ugee Group, Shenzhen, China) with a resolution of 1920 × 1080 pixels at 60 Hz. This device also functioned as the response interface, featuring a pressure-sensitive, battery-free stylus (8192 pressure levels, 5080 LPI resolution, tilt sensitivity). Participants moved the stylus directly on the screen surface, and stylus position and kinematic data were continuously recorded by the MonkeyLogic software at a sampling rate of 1 kHz for later analysis.

Task Design

Participants performed a randomized reach paradigm comprising Delayed Reaction Time (DRT) trials and Simple Reaction Time (SRT) trials. In both trial types, participants began by positioning the stylus at a central fixation point (FP) displayed on an XP-Pen tablet. In the Delayed RT trials, following a 500 ms fixation period, a green peripheral target (a square) appeared at one of two possible locations, while the fixation point remained illuminated for an additional 1000 ms (Hold Time). During this hold period, participants were required to withhold movement despite the target being visible. Participants were instructed to initiate their reaching movement towards the target only after the FP disappeared, which served as the Go cue (Figure 1, left). This delay period allowed us to dissociate target selection and motor preparation processes from movement execution. For Simple RT trials (Figure 1, right), the target onset coincided with the immediate disappearance of the FP, prompting participants to initiate movement as quickly as possible without any imposed delay. This

condition served as a baseline or control for measuring reaction times without an intervening hold period. Both trial types were randomly intermixed in equal proportions throughout each session to prevent anticipatory strategies. Each session comprised 100 experimental trials (50 trials to each of two predefined target positions: ±4.5° horizontal, ±11° vertical from the central FP). Successful target acquisition within a predetermined time window was signalled with an auditory feedback tone (1000 Hz, 100 ms duration). To ensure familiarity with the task requirements and reduce learning effects during data collection, participants completed 20–25 practice trials before beginning the main experimental session.

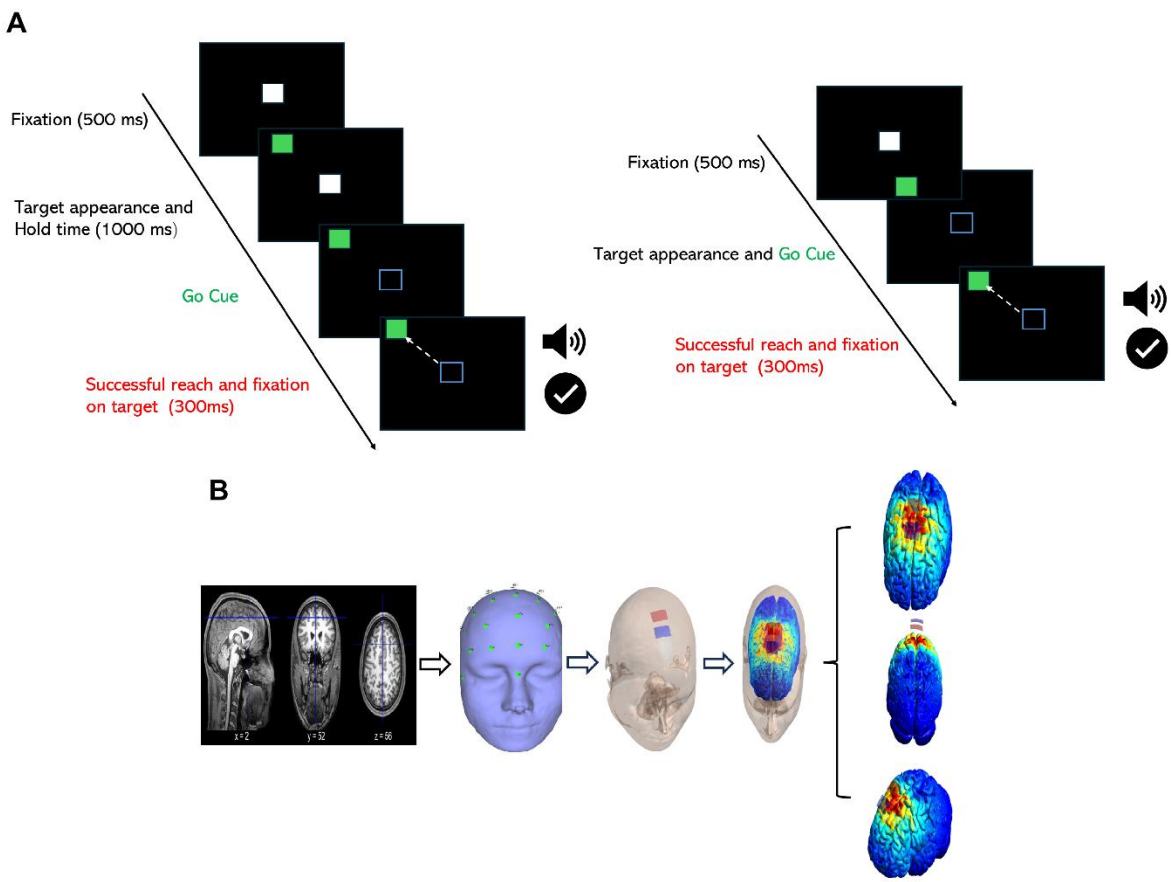

Figure 1. Schematic diagram of experimental paradigm and head modeling. (A) Task design: Delayed Reaction Time trials (left) with fixation, target appearance, and delayed go cue; Simple Reaction Time trials (right) with simultaneous target onset and go cue. (B) Head modeling pipeline: MRI acquisition, 3D reconstruction and tissue segmentation, electrode placement and electric field simulation results showing current density distributions.

tDCS Protocol

Device and Electrode Configuration

Transcranial direct current stimulation was delivered using a 1×1 low intensity stimulator (Model 2004, Soterix Medical Inc). Custom carbon rubber electrodes (3 × 2 cm; surface area 6 cm^2) coated with gel were used to ensure durability, stable conductivity, and improved focality compared to larger sponge electrodes, thereby reducing current spread to adjacent brain regions.

Stimulation location and parameters

For one participant, SMA was localised anatomically from individual T1-weighted MRI scans (1 mm isotropic voxel resolution). The estimated location of the SMA for this participant was estimated as being 1.8 cm anterior to Cz, which was consistent with previous studies (Carlsen et al., 2015; Sadler et al., 2022). Therefore, in the remaining participants, the SMA location was determined using the international 10–20 EEG system, defined as 1.8 cm anterior to Cz. In the anodal condition, the anode was placed over SMA and the cathode over FCz. Stimulation was delivered at 2.0 mA for 10 minutes with 30 s ramp-up and ramp-down. In the sham condition, electrodes were positioned identically, but stimulation was limited to a brief 30 s ramp-up and ramp-down at the start to mimic sensation without the current delivery. After a pre-stimulation behavioural session, participants received stimulation according to protocol, rested for 10 minutes, and then performed the post-stimulation session.

Electric Field and Current Distribution Simulation

With high-resolution T1-weighted MRI scans, a finite element head model was generated using the SimNIBS 4.1 “CHARM” pipeline (Puonti et al., 2020) (Figure 1B). The pipeline segmented scalp, skull, cerebrospinal fluid, gray matter, and white matter, and incorporated diffusion data when available to model tissue anisotropy. Electrode size, location, polarity, and stimulation parameters matched those used in the experiment (2 mA; 3 × 2 cm electrodes; SMA target 1.8 cm anterior to Cz; return at FCz). Head meshes segmented scalp, skull, CSF, gray, and white matter; electrode size, location, and current matched the

experimental setup. Simulations produced spatial maps of induced electric fields (V/m) and current density (A/m²), allowing assessment of focality and peak field magnitude within SMA. (see Figure 1B).

Data Acquisition and Analysis

Behaviour Data

The stylus position was sampled at 1 kHz in Monkey Logic, a MATLAB-based real-time behavioral and data acquisition software developed by NIMH (Hwang et al., 2019). Stylus position data were low-pass filtered using a 5-point moving average with zero-phase distortion. Displacement was computed from filtered *x–y* trajectories; tangential velocity and acceleration were derived by numerical differentiation. Reaction time (RT) was calculated as the interval from the go cue to movement onset, defined as the first time point at which tangential velocity exceeded 10 cm/s. Maximum velocity and maximum acceleration were extracted from the velocity and acceleration profiles, respectively, obtained through sequential differentiation of the position signal. Trials with RT < 100 ms, missed targets, or irregular movement trajectories were excluded from analysis.

EMG Signal recording, Pre-processing, and Motor Unit Analysis

All signal processing, statistical analyses, and visualization were performed using MATLAB (MathWorks, Inc.) with custom-developed algorithms for trial synchronization, spike detection, and PSTH computation. High-density surface EMG signals were acquired at 2000 Hz from a Muovi system (OT Bioelettronica, Italy) using 32 electrodes spaced 5 mm apart, arranged as a grid of 4 rows and 8 columns. The monopolar EMG signals were converted to 28 bipolar channels (4×7) to enhance signal-to-noise ratio and minimize common-mode interference. Raw signals underwent comprehensive preprocessing, including fourth-order Butterworth bandpass filtering (10–500 Hz) followed by line noise removal using standard spectrum estimation techniques. EMG amplitude envelopes were extracted by averaging signals across all channels, then smoothed using a 25 ms temporal window to capture rapid bursts and transient changes during the dynamic reaching task. RMS envelopes were averaged across trials and normalized by dividing by the maximum amplitude observed across both pre- and post-stimulation conditions, yielding values scaled from 0 to 1. This max

normalization approach enabled direct amplitude comparisons across conditions while preserving the relative magnitude of neural excitability changes induced by tDCS, with trials containing missing values excluded to maintain data integrity.

Motor unit spike detection was implemented using adaptive peak detection algorithms with baseline activity computed from a 500 ms post-trial start window. Motor unit detection thresholds were set at 3, 5, and 7 standard deviations from baseline mean to accommodate varying signal amplitudes while minimizing noise (Rungta and Murthy, 2023). Temporal constraints included minimum inter-spike intervals of 40 samples (40 ms), peak width boundaries of 10–40 samples (10–40 ms), and half-prominence width reference to ensure robust motor unit action potential identification. Single-subject peri-stimulus time histograms were constructed for putative small, medium, and large motor units using 10 ms temporal bins (0.01 s). Spike trains were temporally aligned to go cue and movement onset based on the analysis window. PSTH smoothing employed Gaussian convolution with 20 ms (sigma) standard deviation, where the window size was computed and applied using filtfilt processing to prevent temporal distortion. Instantaneous firing rates were calculated as spike counts averaged by trial number and bin duration. Firing rates were further normalized by dividing by the maximum firing rate observed across all trials and conditions for each motor unit type, scaling values from 0 to 1 and enabling standardized comparison of neural recruitment patterns across pre- and post-tDCS conditions. For visualization purposes, raster plots displaying individual spike times were overlaid beneath instantaneous firing rate traces (non-normalized) for visual validation of temporal patterns.

For population-level analysis, motor unit firing rates from all subjects were pooled by motor unit type (small, medium, large) and event alignment. Two distinct 0.5 s analysis windows were examined: a preparatory window spanning 0.5 s immediately preceding the go cue (−0.5 to 0 s relative to go cue onset), and an execution window spanning 0.5 s immediately following movement onset (0 to +0.5 s relative to movement onset). Spike trains within each window were binned at 10 ms resolution, yielding 50 temporal bins per subject per condition. Pooling across all nine subjects generated 450 data points (50 bins × 9 subjects) for each motor unit class and analysis window. To characterize population-wide activity distributions, all subject data were grouped into two independent samples—pre-stimulation and post-stimulation, enabling direct comparison of tDCS-induced shifts in firing rate distributions across the entire cohort within each defined temporal window. This independent-samples design allowed for robust statistical assessment of intervention effects

on both central tendency and variability in motor unit recruitment patterns across subjects. Pooled firing rates were averaged across subjects and normalized by dividing by the maximum firing rate observed within each motor unit type across the entire cohort, scaling all data from 0 to 1 and minimizing the influence of individual baseline variability in firing amplitude. This max normalization strategy preserved the relative magnitude of population-wide neural modulation while enabling standardized statistical comparison of pre- versus post-intervention activity distributions, thereby revealing consistent changes in motor unit recruitment across preparatory and execution epochs following tDCS intervention.

Statistical Analysis

All statistical analyses were performed using MATLAB (MathWorks Inc.) with the Statistics and Machine Learning Toolbox. Data normality was assessed using the Shapiro-Wilk test before analysis selection. Behavioral measures, including reaction time (RT) and peak movement velocity, were analysed using paired comparisons across pre- and post-tDCS sessions within subjects ($n = 9$). Directional hypotheses were evaluated using one-tailed tests: post-tDCS RT was hypothesized to be shorter than pre-tDCS RT, while post-tDCS maximum velocity was hypothesized to exceed pre-tDCS values. Paired-samples *t*-tests were employed for normally distributed data, whereas Wilcoxon signed-rank tests were used for non-normal distributions, with test selection determined by Shapiro-Wilk normality assessment of difference scores. Motor unit firing rates were analysed within two distinct time windows: 500 ms preceding the go cue (−0.5 to 0 s) and 500 ms following movement onset (0 to +0.5 s) for population-level comparisons. Population-level analyses employed hierarchical data pooling, wherein individual subject firing rates were concatenated across subjects within each motor unit size class (small, medium, large) to form two independent samples, pre-stimulation (450 data points) and post-stimulation (450 data points) maximizing statistical power while preserving physiological motor unit architecture. Pre- versus post-tDCS intervention comparisons at the single-subject level were conducted using Wilcoxon signed-rank tests (one-tailed) for paired trial-by-trial comparisons within subjects. Population-level group comparisons utilized Wilcoxon rank-sum tests (Mann-Whitney U tests) to evaluate the directional hypothesis that post-intervention firing rate distributions exceeded pre-intervention levels across the pooled cohort. This independent-samples approach tested whether the two distributions differed systematically, with the test statistic based on rank sums calculated from the combined 900 data points (450 pre + 450 post) per motor unit type and temporal window. Statistical significance was set at $\alpha = 0.05$ for all analyses. Effect sizes

were calculated as rank-biserial correlation coefficients (r) for non-parametric analyses and Cohen's d for parametric tests to provide standardized measures of treatment magnitude. Pearson product-moment correlation coefficients were computed to assess linear relationships between changes in motor unit activity and changes in behavioral hold time metrics for all three putative motor unit sizes (small, medium, and large), with statistical significance evaluated at $\alpha = 0.05$. All statistical tests were one-tailed unless otherwise specified, with exact p-values, test statistics (t or z-scores), effect sizes (d or r), and sample sizes (n) reported throughout

Results

Behavioral and Kinematic Performance improved on tDCS SMA.

A total of nine subjects were included in the test group and seven subjects in the control group for analyses of reaction time and maximum velocity in the randomised reaching task ($n = 9$ test, $n = 7$ control). In the test group, reaction time was markedly improved, with mean pre-stimulation RT of 204.08 ms (SD = 36.26) and mean post-stimulation RT of 188.42 ms (SD = 28.05), yielding a mean paired difference of −15.66 ms (SD = 16.69; Shapiro–Wilk $p = 0.823$; $t(8) = -2.82$, $p = 0.011$; one-sided 95% CI = [−∞, −5.32] ms; Cohen's $d = -0.939$; Power = 0.822). By contrast, the control group did not show a significant change in behavioral response speed. (see Figure 2A). Parallel improvements were observed in kinematic performance. The test group demonstrated a significant elevation in maximum velocity during reaching movements, with mean pre-stimulation velocity of 45.69 cm/s (SD = 9.18) and mean post-stimulation velocity of 48.11 cm/s (SD = 10.76), yielding a mean paired difference of 2.42 cm/s (SD = 2.45; Shapiro–Wilk $p = 0.339$; $t(8) = 2.96$, $p = 0.009$; one-sided 95% CI = [0.90, ∞) cm/s; Cohen's $d = 0.987$; Power = 0.854). Conversely, the control group did not exhibit a significant shift in kinematic parameters. Taken together, these data highlight that the tDCS intervention specifically improved both the rapid initiation and execution velocity of reaching movements in the test group, with no comparable advances occurring in the control group. (see Figure 2B)

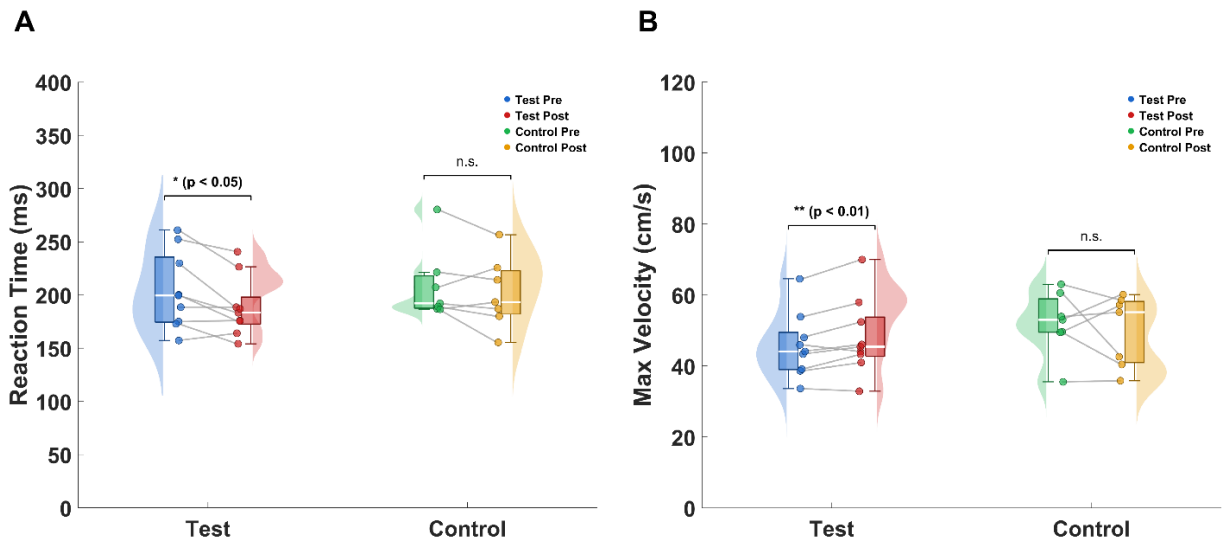

Figure 2. **tDCS intervention effects on behavioral and kinematic performance in the delayed reach task.** (A), Behavioral performance: Reaction time changes from pre- to post-intervention. Test group (n=9) showed significant reduction in response latency while the control group (n=7) showed no significant change (n.s.). (B), Kinematic performance: Maximum velocity changes from pre- to post-intervention. Test group demonstrated a significant increase in movement execution speed while the control group showed no significant change (n.s.). Individual participant data are connected by lines, while box plots show the median and quartiles, and violin plots display the data distribution. Asterisks indicate statistical significance levels.

Spatial selectivity of EMG and motor unit activity during delayed reaching movements

EMG responses from all participants (n = 9) across all trials were analysed to examine preparatory muscle activity in the anterior deltoid during the randomized delayed reach task. Normalized RMS EMG averaged across participants and aligned to the Go cue showed robust activation in In-RF trials (target at −4.5°, +11°) following the Go cue, but minimal preparatory activity during the delay period, consistent with prior reports that conventional EMG cannot detect preparatory activities (Figure 3A). In contrast, decomposition of high-density EMG into putative small, medium, and large amplitude motor units revealed that small amplitude/small-threshold motor units exhibited selective, sustained firing during the delay period in In-RF trials (normalized firing rate rising much before Go cue), while remaining quiescent in Out-RF trials (target at +4.5°, −11°), demonstrating spatially tuned preparatory recruitment (Figure 3B). Medium and large motor units showed minimal delay activity but vigorous post-Go cue firing in In-RF trials, consistent with size-principle recruitment during movement execution. These findings demonstrate that preparatory activity missed by conventional RMS EMG is revealed by threshold-based detection of low-threshold motor units using high-density surface EMG, confirming that preparatory motor drive reaches the peripheral level through selective, context-specific recruitment undetectable by single-channel or low-density recording methods used in previous studies.

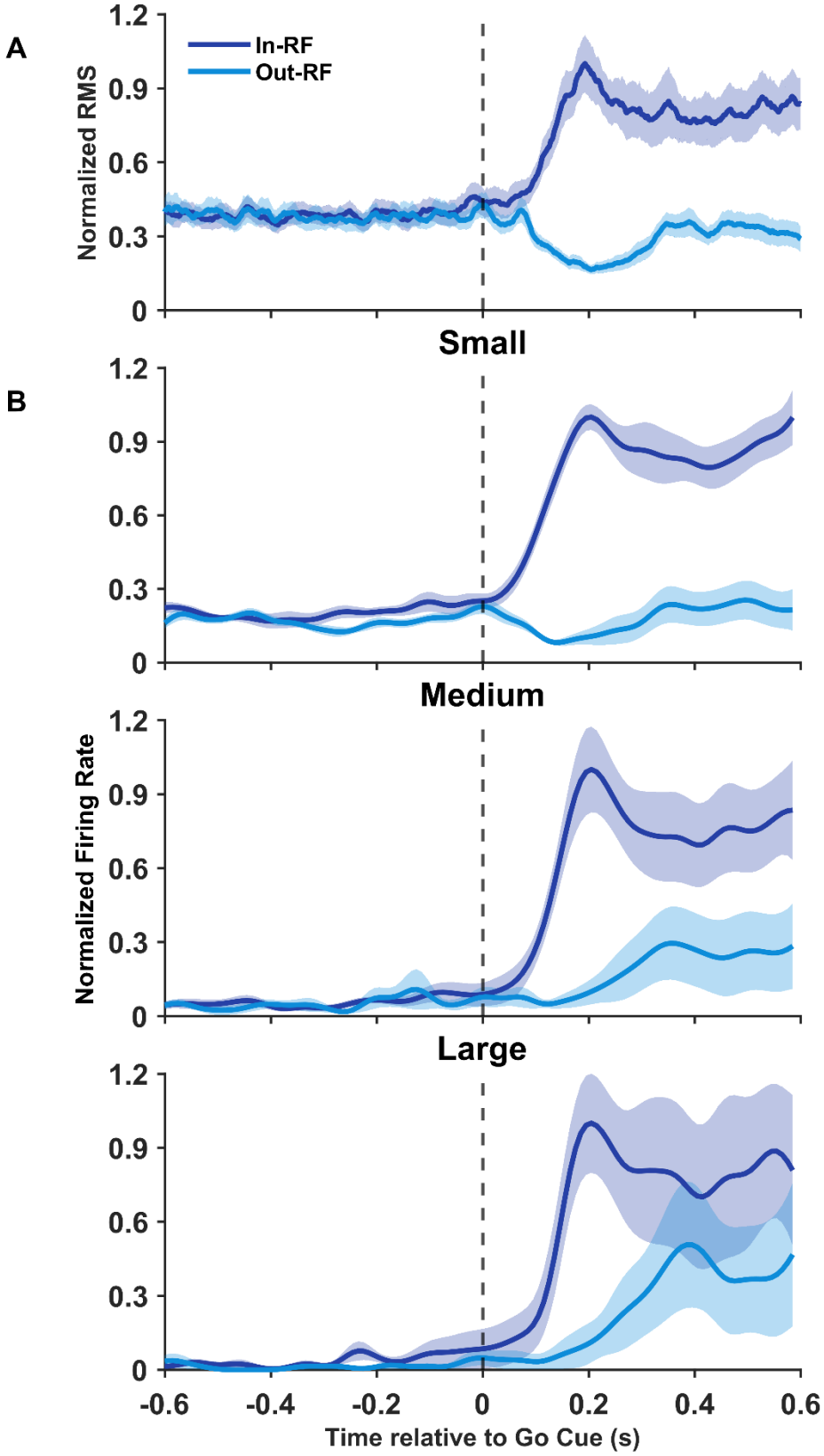
A
B
In-RF
Out-RF
Normalized RMS
Small
Medium
Large
Normalized Firing Rate
1.2
0.9
0.6
0.3
0
-0.6
-0.4
-0.2
0
0.2
0.4
0.6
Time relative to Go Cue (s)

Figure 3. Spatial selectivity of the total EMG and motor unit related activity during the delayed reaching task. (A)Normalized root-mean-square (RMS) EMG activity from the anterior deltoid averaged across all participants (n = 9) and aligned to the Go cue (vertical dashed line at t = 0 in each panel). (Dark blue) trace represents trials within the muscle's response field (In-RF; target at −4.5°, +11°), showing robust activation following the Go cue. (Light blue) trace represents trials outside the response field (Out-RF; target at +4.5°, −11°), showing minimal EMG activity. (B) Normalized motor unit related activity for small, medium, and large threshold motor units across (n = 9) displayed as peri-stimulus time histograms (PSTHs). Small amplitude motor units exhibit selective, sustained activity during the delay period in In-RF trials (Dark blue) while remaining relatively quiescent in Out-RF trials (Light blue), demonstrating spatially tuned preparatory recruitment. Medium and large motor units show minimal delay-period activity in both In-RF and Out-RF conditions but vigorous post-Go cue firing selectively in In-RF trials. Thick lines represent mean; shaded regions denote ± standard error of the mean (SEM). All data were averaged across subjects and then normalised by the peak activity.

tDCS over SMA enhances preparatory motor unit activity and movement execution activity.

EMG data from a single subject were analysed using $N = 22$ trials for each pre- and post-tDCS condition. All activities were normalized to the maximal amplitude observed across both pre- and post-stimulation conditions (expressed in microvolts), following established normalization procedures for between-condition comparisons. Normalized values are reported as proportions of this maximum.

Normalized RMS EMG amplitudes (Figure 4A) showed stable resting activity with selective, stimulation-linked increases during task phases for in–RF trials. A one-tailed Wilcoxon signed-rank test was used to assess whether post-stimulation values exceeded pre-stimulation across trial-level window means.At baseline (−1 to −0.5 s), normalized amplitudes were comparable pre- versus post-tDCS (pre mean = 0.326, SD = 0.029; post mean = 0.284, SD = 0.018; median difference = −0.070), indicating preserved resting tone ($p = 0.865$, $z = -1.104$, $r = 0.24$, small effect). During movement preparation (−0.5 to 0 s), normalized RMS remained stable after stimulation (pre mean = 0.328, SD = 0.024; post mean = 0.312, SD = 0.029; median difference = −0.051; $p = 0.577$, $z = -0.195$, $r = 0.04$, negligible effect), consistent with maintained pre-movement readiness similar to baseline and no early

build up. During early response or planning phase (0 to 0.2 s), a pronounced post-tDCS increase in normalized values was observed, shifting from pre mean = 0.514 (SD = 0.228) to post mean = 0.666 (SD = 0.190), with a median difference of 0.275; $p = 0.030$, $z = 1.883$, $r = 0.40$ (medium effect), reflecting facilitated motor execution (see Figure 4A).

Complementing these EMG findings, motor unit firing rates were evaluated across small, medium, and large recruitment threshold motor units during the preparatory period (−0.5 to 0 s; $N = 22$ paired trials per unit type). All firing rates were normalized to the maximal firing rate observed for each motor unit across both pre- and post-stimulation conditions (small: 40.91 sp/s; medium: 26.29 sp/s; large: 15.64 sp/s), reported as proportions of this maximum (see Figure 4B).Small motor units exhibited a significant increase in normalized firing rate following tDCS (pre mean = 0.122, SD = 0.269; post mean = 0.237, SD = 0.207; median difference = 0.189; $p = 0.014$, $z = 2.203$, $r = 0.56$, large effect). Medium-threshold units remained stable (pre mean = 0.064, SD = 0.281; post mean = 0.060, SD = 0.182; median difference = 0.000; $p = 0.924$, $z = 1.433$, $r = 0.45$, medium effect). Large-threshold motor units showed no significant change (pre mean = 0.043, SD = 0.203; post mean = 0.038, SD = 0.155; median difference = 0.000; $p = 0.923$, $z = 1.423$, $r = 0.53$, large effect). Taken together, the RMS EMG and motor unit analyses converge to indicate preserved baseline activity with SMA stimulation-related enhancement of preparatory and early response motor unit activity, particularly for the smaller motor unit activity, for a single subject (see Figure 4B).

Extending these findings across the cohort, pooled population-level analysis (see Methods section) demonstrated robust and significant tDCS-induced increases in motor unit excitability during the preparatory window preceding the go cue ($n = 9$ subjects, 450 data points per condition). All firing rates were normalized to the maximal firing rate observed for each motor unit type across both conditions (small: 33.68 sp/s; medium: 19.67 sp/s; large: 12.89 sp/s), reported as proportions of this maximum (see Figure 4C). When all subjects' data were normalized and analysed collectively using Wilcoxon rank-sum tests, post-tDCS firing rates were significantly higher for small motor units (pre mean = 0.198, SD = 0.085; post mean = 0.225, SD = 0.105; median difference = 0.011; $p = 0.002$, $z = 2.960$, $r = 0.10$, small effect), confirming the individual trend at the group level. Medium motor units exhibited an even stronger group effect (pre mean = 0.055, SD = 0.072; post mean = 0.079, SD = 0.079; median difference = 0.020; $p < 0.001$, $z = 5.306$, $r = 0.18$, small effect). Large motor units also showed pronounced enhancement following tDCS (pre mean = 0.033, SD = 0.093; post

mean = 0.055, SD = 0.090; median difference = 0.006; $p < 0.001$, $z = 5.925$, $r = 0.20$, small effect). These results highlight a consistent population-wide increase in normalized motor unit firing rates in preparation for movement, with effect sizes progressively increasing from small ($r = 0.10$) to medium ($r = 0.18$) to large threshold motor units ($r = 0.20$), supporting a graded excitatory influence of tDCS intervention on neuromuscular activation during the preparatory phase (see Figure 4C).

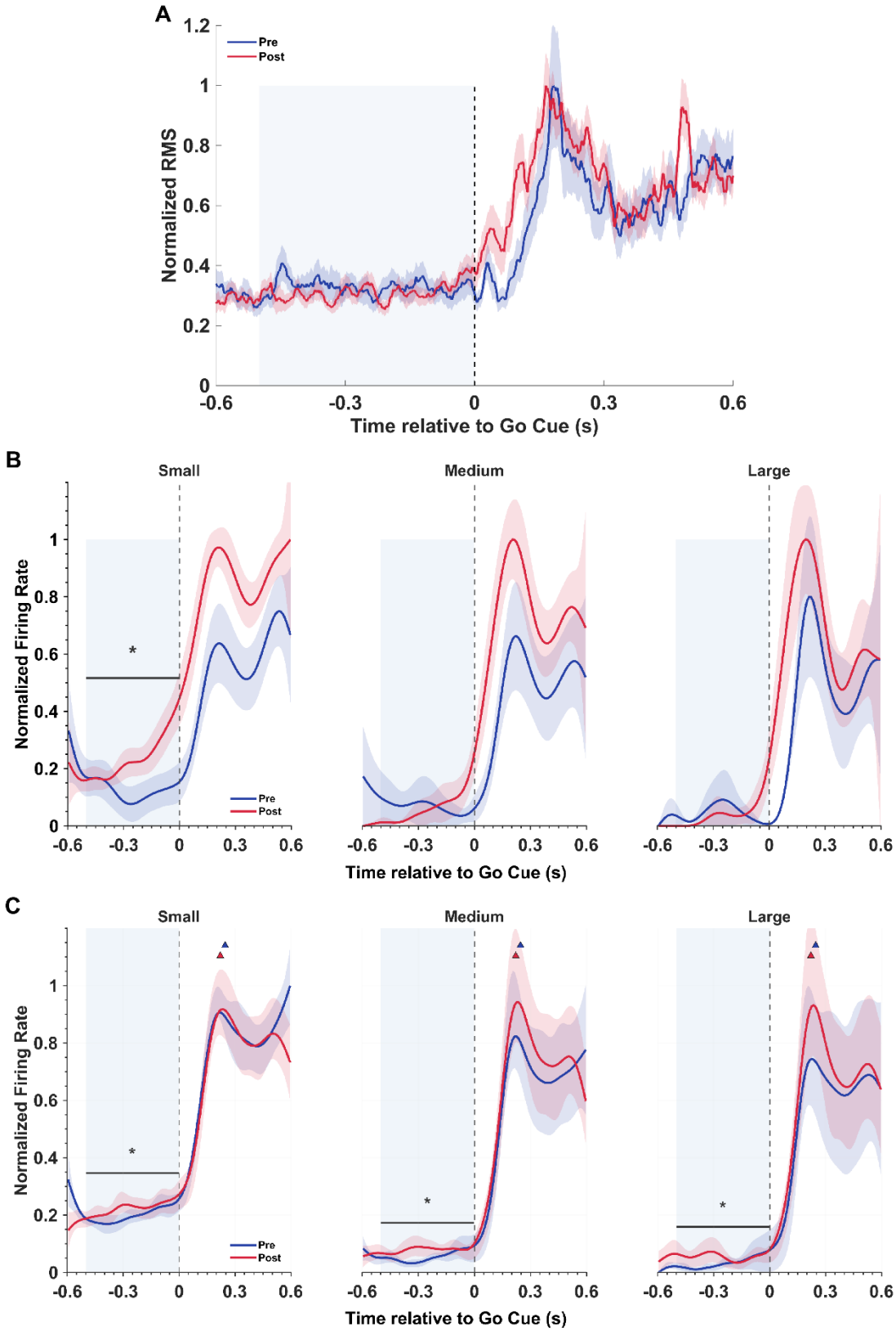

Figure 4. Stimulation-linked changes in normalised RMS EMG and motor unit activity at single-subject and population levels. (A, B) Single-subject data (n = 22 paired Pre-stimulation and Post-stimulation in-RF trials). (A) Normalised RMS EMG traces (mean ±

SEM) time-locked to the Go cue (vertical dashed line); Pre-stimulation = blue, Post-stimulation = red. (B) Normalized motor unit firing rates (mean ± SEM) for small, medium, and large amplitude motor units aligned to the same Go cue; the light blue band marks the preparatory window (−0.5 to 0.0 s). A horizontal bar with an asterisk within the preparatory window marks a significant post-stimulation > pre-stimulation difference for the low threshold, small amplitude motor units. (C) Population-level normalized firing rate traces (mean ± SEM) for small, medium, and large threshold motor units aligned to the Go cue (vertical dashed line; n = 9 subjects, 450 data points per condition); pre-stimulation = blue, post-stimulation = red. The light blue band marks the preparatory window (−0.5 to 0.0 s). Horizontal brackets with asterisks indicate intervals of significant post-stimulation > re-stimulation differences. Triangles denote movement onset (group averages; color-matched to pre-stimulation or post-stimulation condition). Abbreviations: RMS, root mean square; SEM, standard error of the mean. (see the method section for the detailed explanation of the method used in this cohort analysis).

Robust high- threshold motor unit firing dynamics during movement execution phase.

Given the behavioral evidence of significantly enhanced maximum velocity post-tDCS (Figure 2B), motor unit firing rates were further evaluated during the movement execution window (0 to 0.5 s aligned to movement onset; n = 9 subjects, 450 data points per condition). All firing rates were normalized to the maximal firing rate observed for each motor unit type across both conditions (small: 35.46 sp/s; medium: 20.11 sp/s; large: 13.78 sp/s), reported as proportions of this maximum. Small motor units did not show a significant change in normalized firing rate after tDCS (pre mean = 0.835, SD = 0.270; post mean = 0.821, SD = 0.291; median difference = 0.009; p = 0.647, z = −0.377, r = −0.01, negligible effect), suggesting that tDCS effects on these low-threshold motor units may be more pronounced in movement preparation than during execution. In contrast, both medium and large motor units exhibited significant post-tDCS increases in normalized firing rates during the execution phase, with medium units showing a modest increase (pre mean = 0.740, SD = 0.500; post mean = 0.793, SD = 0.484; median difference = 0.045; p = 0.041, z = 1.739, r = 0.06, negligible effect). Large motor units showed the most pronounced enhancement (pre mean = 0.660, SD = 0.682; post mean = 0.728, SD = 0.603; median difference = 0.222; p = 0.008, z = 2.419, r = 0.08, negligible effect), indicating that during actual movement, the excitatory

effects of tDCS become more prominent in higher-threshold motor unit pools, which are critically involved in generating greater movement velocities.

Relationship between motor unit modulation and the hold time effect.

To assess whether tDCS-induced neural modulation of muscle activity in (Figure 4A,B,C) was related to behavioral preparation in (Figure 2A) leading to the hold time effect, we also correlated delta motor unit activity (post-minus-pre changes in average firing rates) with delta hold time defined as [Post(delayed RT – simple RT)] − [Pre(delayed RT – simple RT)] for each subject, where hold time measures the preparatory interval from target appearance to go cue. Across subjects, small ($r = -0.298$, $p = 0.436$), medium ($r = -0.367$, $p = 0.331$), and large motor units ($r = -0.547$, $p = 0.127$) all showed non-significant negative correlations, indicating a trend toward greater increases in motor unit activity accompanying larger reductions in preparatory hold time, though the relationships did not reach statistical significance. (see Figure 5)

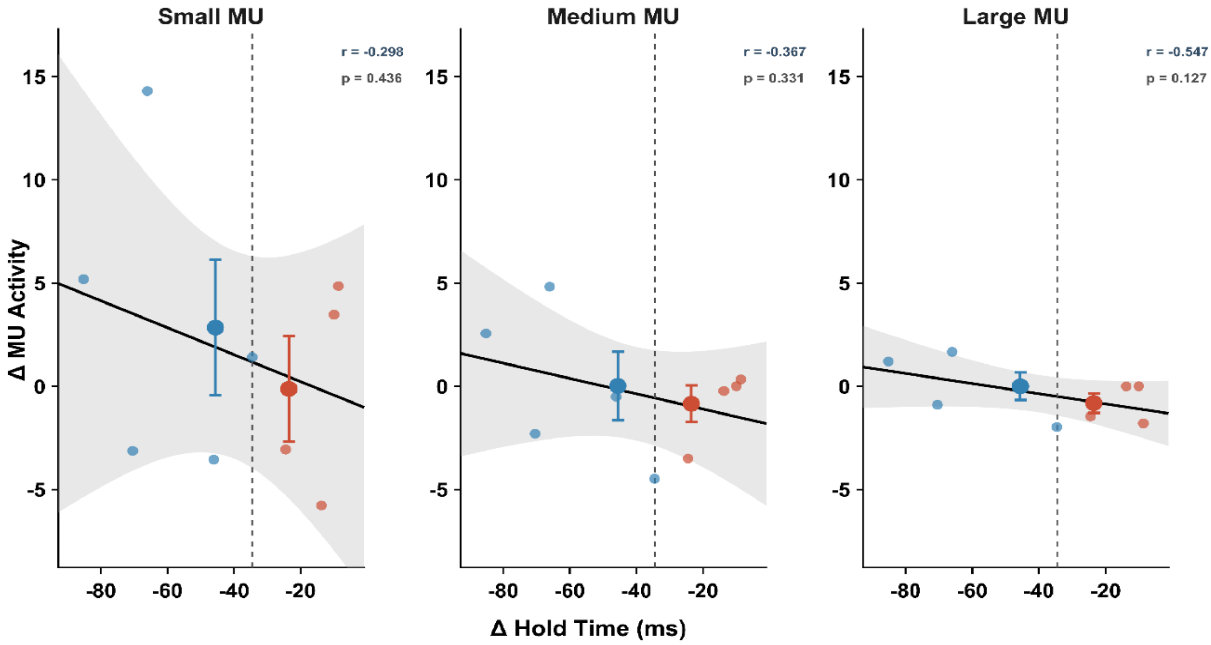

Figure 5. Correlation between motor unit activity changes and preparatory behavior. Scatter plots showing the relationship between changes in motor unit firing rate (Δ motor unit activity, post-stimulation minus Pre-stimulation) and changes in hold time (Δ hold time) for small, medium, and large motor unit pools ($n = 9$ subjects). Individual subjects are

represented by individual data points, color-coded by median split: blue = subjects with more negative Δ hold time (greater hold time reduction); red = subjects with less negative Δ hold time (smaller hold time reduction). Larger symbols with error bars denote cohort mean ± SEM for each subgroup. Solid regression lines indicate Pearson correlation fits with 95% confidence interval shading. Vertical dashed line marks the median split of Δ hold time (See last para of results section). Abbreviations: Δ, change (post-stimulation minus Pre-stimulation); SEM, standard error of the mean.

Discussion

To the best of our knowledge this is the first attempt at investigating the peripheral signature of motor preparation induced by neuromodulation of the supplementary motor area (SMA). In a randomised delayed reaching task, anodal stimulation of the SMA enhanced both motor preparation and downstream execution, shortening reaction times and elevating preparatory and planning-phase RMS EMG activity without increasing baseline discharge. These findings demonstrate that preparatory activity is also enhanced in the motor unit activity, whereas the transition into the planning and execution phase, particularly during movements with greater peak velocity, recruits and modulates medium- and higher-threshold motor units (medium and larger) more strongly. This progressive recruitment pattern suggests that SMA-targeted tDCS augments early preparatory neural drive while simultaneously facilitating the higher-force activation required for improved movement execution. Collectively, the converging behavioral and EMG evidence reveals that SMA neuromodulation amplifies a peripheral "preparatory set."

Relation to previous work

Prior work has established that neurons in the SMA exhibit delay-period activity that anticipates movement and distinguishes preparation from execution, since they show little or no activity in the latter phase. These studies have framed the SMA as a controller of the preparatory set that biases motor circuits toward imminent action (Tanji, 1984; Tanji, 1994). In addition, prior EMG studies have mostly concluded that preparation was centrally confined because no overt muscle activity was detected during delays, a conclusion shaped by the sensitivity limits of single-channel EMG, coarse filters, and a focus on gross agonist

activation rather than low-amplitude unit behavior (Tanji & Evarts, 1976) that was hard to distinguish from baseline EMG noise. Subsequent behavioral neuromodulation work showed that increasing SMA excitability with anodal tES/tDCS can shorten reaction times in a polarity-dependent manner, consistent with shifting the preparatory state closer to an initiation threshold (Carlsen et al., 2015 and others). Together, these strands suggested a cortical preparatory mechanism with behavioral relevance but lacked a clear peripheral signature at the motor unit scale, which we have tested in this study.

One potential limitation in previous EMG related studies which tested muscle activity during motor preparation, was the use of conventional EMG involving electrodes spaced at long distances which would have filtered small, local voltage fluctuations caused by activation of smaller motor units (Tanji and Evarts,1976). In addition, the use of standard signal processing approaches that emphasizes the analogue force related EMG activity such as RMS causes temporal low pass filtering of the EMG signal, emphasizing the whole muscle activity over earlier and smaller preparatory phase of the EMG signal. Furthermore, the use of more distal musculature involving wrist muscles ((Tanji and Evarts, 1976; Tanji & Kurata, 1982,1985), as well as using tasks involving cursor/joystick motion might have restricted the extent of physical movement as well (Prut and Fetz,1999), and produced delayed activity relative to reach onset due to the well-known temporal gradient of proximal to distal muscle related neural activity seen in the motor cortex (Jeannerod, 1981).

These potential limitations have been addressed in the recent work using high-density surface EMG (Rungta and Murthy, 2023). They reported context-specific early recruitment of small amplitude motor units during the delay, topographically tuned to target direction and predictive of reaction times, thereby revealing a peripheral correlate of central preparation that remains subthreshold for overt movement. Methodologically, their use of dense grids, bipolar derivations, and unit-scale spike detection overcame limitations of earlier EMG approaches that averaged away sparse, low-threshold firing which can also be observed in the current study by comparing Figure 4A and B. Conceptually, they argued that a modest, spatially specific increase in descending drive can selectively bias small motor units, preconfiguring the neuromuscular apparatus for rapid initiation without violating no movement constraints during the hold period. These conclusions appear justified and converge with the findings of (Mellah et al.,1990), who first showed the activation of motor units that are selective during motor preparation but not during the execution of delayed movements in monkeys using needle EMG electrodes.

Mechanisms underlying stimulation induced changes in the motor periphery during the delayed period.

The current findings converge with and extend (Rungta and Murthy, 2023) on three fronts. First, behaviorally, anodal SMA stimulation further shortened reaction times in prepared trials (hold time), aligning with a causal role for SMA in configuring a launch-ready state. Second, planning EMG RMS increased (see figure 4A) without baseline elevation, and RF-specific small motor unit discharge rose during the delay (see figure 4B and C), closely mirroring the early recruitment signature described by Rungta and Murthy but now under targeted SMA neuromodulation. Third, during execution, medium/large units showed the most prominent gains, consistent with recruitment principles as described by Henneman (1957) and Henneman et al. (1965), whereby enhanced central drive propagates to higher threshold pools once initiation occurs (see figure 4C and execution part in the results section). This pattern links SMA level causal manipulation to the specific peripheral phenotype predicted by Rungta and Murthy, directly bridging central preparatory dynamics and neuromuscular readiness.

SMA stimulation in this study produced three phase-specific effects: selective RF-specific elevation of delay period activity particularly seen in small -motor unit activity (see figure 4B) with unchanged baseline, faster initiation, and disproportionately greater execution phase recruitment of medium/large motor units. Within Rungta and Murthy's framework, the delay period increase, particularly in -small unit activity indexes a peripheral preparatory set as these motor units are- context-specific that encodes future kinematic or postural states of the muscle and distinguish In-RF vs. Out-RF (see figure 3B), and a bias that predicts reaction time, thereby explaining the rise in preparatory/planning RMS without movement and a shift toward higher threshold- recruitment during movement execution. Extending this model to circuitry, the findings are consistent with the SMA and premotor cortex being a critical part of the preparatory subspace which, being movement null, prevents activation of the primary motor cortex (Kauffmann et al., 2014). This notwithstanding, we suggest that preparatory neural subspaces may encode desired future postures of relevant muscles (Kaufmann et al., 2014), which are conveyed possibly via reticulospinal pathways to spinal gamma motor neurons (Kearsley et al.,2021), yielding early, low-threshold motor-unit activity during the preparatory phase (Rungta & Murthy, 2023; Mellah et al.,1990). Although such gamma

activation on its own would not cause muscle contraction, it could underlie a preparatory set in muscles that subsequently modulates alpha motoneurons via spindle-based feedback, consistent with equilibrium-point/referent-configuration models (Feldman, 1966; Feldman, 1986; Latash, 2010; Bizzi et al., 1982). This latter feedback could be the basis of both shorter reaction times as well as faster muscle contraction, leading to increased vigour of movement we observed. (Hasnain et al.,2025) in a recent study (pre-print) support this division by showing that preparatory and execution components reside in separable neural manifolds that couple to distinct descending channels, offering a principled bridge from cortical subspace dynamics to the peripheral signatures observed here. This layered pathway explains the pattern observed here: delay period- small motor unit engagement, faster initiation, and amplified execution phase- recruitment, and predicts that selective modulation of reticulospinal drive will scale preparatory EMG topographies and movement vigor, whereas corticospinal activation will directly increase alpha motor unit activity via -high threshold motor unit recruitment leading to muscle contraction.

Methodological Issues

The apparent absence of preparatory muscle activity in the previous work can be reconciled with the present and (Rungta and Murthy, 2023) results by considering sensitivity, resolution, and the signal processing analysis that was used. EMG from large and well separated electrodes with coarse temporal smoothing is ill-suited to detect sparse, low amplitude discharges of small units during movement preparation; averaging across channels and trials further suppresses these signals. In contrast, high-density grids (HD-EMG), bipolar spatial filtering of electrodes that are 5mm apart, spike scale detection, and windowed analyses using peristimulus time histograms, centred on the delay capture subtle, context-specific changes that do not manifest as bulk activation. Thus, the older inference that “preparation is purely central” largely reflects measurement constraints rather than a true absence of peripheral modulation. Nevertheless, the current study is not without its limitations. The sample size and cross-subject aggregation limited power resulting in correlations between motor unit activity and hold time that were directionally consistent but non-significant. The electric field targeting SMA was not individualized and is the spread to adjacent medial premotor regions cannot be excluded. Activation of the anterior pre-SMA, which is an inhibitory node, may in fact had the unintended consequence of suppressing muscle activation. The motor unit class

attribution relied on a threshold amplitude rather than full decomposition and longitudinal unit tracking was not attempted. As such, these threshold crossing are still putative motor units and motor unit size maybe conflated with distance of the motor units from the electrode grid. Further, potential confounds such as expectancy from having a fixed hold time, and subtle posture changes during the hold time were controlled indirectly but not exhaustively. We hope to control for these limitations in the future.

Summary and Conclusions

While Tanji's cortical delay period activity in SMA neurons defined the origin of the preparatory set, Carlsen's polarity-dependent RT modulation established a causal leverage at SMA. While the measurement of motor unit excitability indicated that preparatory drive could influence peripheral elements without overt motion Mellah, Rungta and Murthy localized this influence to selective, context-specific recruitment of smaller motor units detectible with high-density surface EMG. The present study unifies these strands by showing that targeted SMA neuromodulation enhances precisely this peripheral preparatory signature and accelerates initiation, articulating a mechanistic bridge from cortical preparation to neuromuscular readiness and its distinct relationship to subsequent execution.

References:

1. Shenoy, K. V., Sahani, M., & Churchland, M. M. (2013). Cortical control of arm movements: A dynamical systems perspective. Annual Review of Neuroscience, 36, 337–359. https://doi.org/10.1146/annurev-neuro-062111-150509

2. Churchland, M. M., Cunningham, J. P., Kaufman, M. T., Foster, J. D., Nuyujukian, P., Ryu, S. I., & Shenoy, K. V. (2012). Neural population dynamics during reaching. Nature, 487(7405), 51–56. https://doi.org/10.1038/nature11129

3. Elsayed, G. F., Lara, A. H., Kaufman, M. T., Churchland, M. M., & Cunningham, J. P. (2016). Reorganization between preparatory and movement population responses in motor cortex. Nature Communications, 7, 13239. https://doi.org/10.1038/ncomms13239

4. Picard, N., & Strick, P. L. (1996). Motor areas of the medial wall: A review of their location and functional activation. Cerebral Cortex, 6(3), 342–353. https://doi.org/10.1093/cercor/6.3.342

5. Nachev, P., Kennard, C., & Husain, M. (2008). Functional role of the supplementary and pre-supplementary motor areas. Nature Reviews Neuroscience, 9(11), 856–869. https://doi.org/10.1038/nrn2478

6. Tanji, J. (1984). The neuronal activity in the supplementary motor area of primates. Trends in Neurosciences, 7(12), 439–441. https://doi.org/10.1016/0166-2236(84)90196-4[6]

7. Cunnington, R., Windischberger, C., Deecke, L., & Moser, E. (2002). The preparation and execution of self-initiated and externally-triggered movement: A study of event-related fMRI. NeuroImage, 15(2), 373–385. https://doi.org/10.1006/nimg.2001.0976

8. Jenkins, I. H., Jahanshahi, M., Jueptner, M., Passingham, R. E., & Brooks, D. J. (2000). Self-initiated versus externally triggered movements. II. The effect of movement predictability on regional cerebral blood flow. Brain, 123(6), 1216–1228. https://doi.org/10.1093/brain/123.6.1216

9. Shibasaki, H., & Hallett, M. (2006). What is the Bereitschaftspotential? Clinical Neurophysiology, 117(11), 2341–2356. https://doi.org/10.1016/j.clinph.2006.04.025

10. Lau, H. C., Rogers, R. D., Haggard, P., & Passingham, R. E. (2004). Attention to intention. Science, 303(5661), 1208–1210. **https://doi.org/10.1126/science.1090973**

11. Tanji, J., & Shima, K. (1994). Role for supplementary motor area cells in planning several movements ahead. Nature, 371(6496), 413–416. **https://doi.org/10.1038/371413a0**

12. Shima, K., & Tanji, J. (2000). Neuronal activity in the supplementary and presupplementary motor areas for temporal organization of multiple movements. Journal of Neurophysiology, 84(4), 2148–2160. **https://doi.org/10.1152/jn.2000.84.4.2148**

13. Tanji, J. (2001). Sequential organization of multiple movements: Involvement of cortical motor areas. Nature Reviews Neuroscience, 2(8), 599–607. **https://doi.org/10.1038/35090056**

14. Deecke, L., & Kornhuber, H. H. (1978). An electrical sign of participation of the mesial "supplementary" motor cortex in human voluntary finger movement. Brain Research, 159(2), 473–476. **https://doi.org/10.1016/0006-8993(78)90561-9[14**]

15. Colebatch, J. G. (2007). Bereitschaftspotential and movement-related potentials: Origin, significance, and application in disorders of human movement. Movement Disorders, 22(5), 601–610. **https://doi.org/10.1002/mds.21323**

16. Churchland, M. M., Santhanam, G., & Shenoy, K. V. (2006). Preparatory activity in premotor and motor cortex reflects the speed of the upcoming reach. Journal of Neurophysiology, 96(6), 3130–3146. **https://doi.org/10.1152/jn.00307.2006**

17. Churchland, M. M., Cunningham, J. P., Kaufman, M. T., Ryu, S. I., & Shenoy, K. V. (2010). Cortical preparatory activity: representation of movement or first cog in a dynamical machine? *Neuron*, *68*(3), 387–400. **https://doi.org/10.1016/j.neuron.2010.09.015**

18. Lara, A. H., Cunningham, J. P., & Churchland, M. M. (2018). Different population dynamics in the supplementary motor area and motor cortex during reaching. Nature Communications, 9(1), 2754. **https://doi.org/10.1038/s41467-018-05146-z**

19. Carlsen, A. N., Chua, R., Inglis, J. T., Sanderson, D. J., & Franks, I. M. (2015). Transcranial direct current stimulation over the supplementary motor area modulates

preparatory processes and movement initiation. Neuroscience Letters, 591, 21–26. https://doi.org/10.1016/j.neulet.2015.02.010

20. Sadler, C. M., Holmes, P. S., & Celnik, P. A. (2021). Transcranial direct current stimulation of supplementary motor area enhances upper limb movement in Parkinson's disease. Clinical Neurophysiology, 132(9), 2162–2171. https://doi.org/10.1016/j.clinph.2021.05.025

21. Tanji, J., & Evarts, E. V. (1976). Anticipatory activity of motor cortex neurons in relation to direction of an intended movement. Journal of Neurophysiology, 39(5), 1062–1068. https://doi.org/10.1152/jn.1976.39.5.1062

22. Rungta, S., & Murthy, A. (2023). Context-specific early recruitment of small motor units in the shoulder muscle reflects a reach decision. Journal of Neurophysiology, 129(6), 1443–1463. https://doi.org/10.1152/jn.00522.2022

23. Hwang, J., Mitz, A. R., & Murray, E. A. (2019). NIMH MonkeyLogic: Behavioral control and data acquisition in MATLAB. Journal of Neuroscience Methods, 323, 13–21. https://doi.org/10.1016/j.jneumeth.2019.05.002

24. Puonti, O., Van Leemput, K., & Thielscher, A. (2020). Accurate and robust whole-head segmentation from magnetic resonance images for individualized head modeling. NeuroImage, 219,117046. https://doi.org/10.1016/j.neuroimage.2020.117046

25. Feldman, A. G. (1966). Functional tuning of the nervous system with control of movement or maintenance of a steady posture: II. Adjustable parameters in muscles. Biophysics, 11, 565–578. https://pubmed.ncbi.nlm.nih.gov/5999810/

26. Feldman, A. G. (1986). Once more on the equilibrium-point hypothesis (lambda model) for motor control. Journal of Motor Behavior, 18(1), 17–54. https://doi.org/10.1080/00222895.1986.10735369

27. Latash, M. L. (2010). Motor synergies and the equilibrium-point hypothesis. Motor Control, 14(3), 294–322. https://doi.org/10.1123/mcj.14.3.294

28. Bizzi, E., Accornero, N., Chapple, W., & Hogan, N. (1982). Arm trajectory formation in monkeys. Experimental Brain Research, 46(1), 139–143. https://doi.org/10.1007/BF00238107

29. Mellah, S., Rispal-Padel, L., & Riviere, G. (1990). Changes in excitability of motor units during preparation for movement. Experimental Brain Research, 82(1), 178–186. **https://doi.org/10.1007/BF00230849**

30. Crammond, D. J., & Kalaska, J. F. (2000). Prior information in motor and premotor cortex: activity during the delay period and effect on pre-movement activity. *Journal of neurophysiology*, *84*(2), 986–1005. **https://doi.org/10.1152/jn.2000.84.2.986**

31. Jeannerod, M. (1981). Intersegmental coordination during reaching at natural visual objects. In J. Long & A. Baddeley (Eds.), Attention and performance IX (Vol. 9, pp. 153–168). Lawrence Erlbaum Associates

32. Prut, Y., & Fetz, E. E. (1999). Primate spinal interneurons show pre-movement instructed delay activity. *Nature*, *401*(6753), 590–594. **https://doi.org/10.1038/44145**

33. Sato, T., Katagiri, N., Suganuma, S., Laakso, I., Tanabe, S., Osu, R., Tanaka, S., & Yamaguchi, T. (2024). Simulating tDCS electrode placement to stimulate both M1 and SMA enhances motor performance and modulates cortical excitability depending on current flow direction. *Frontiers in Neuroscience*, 18, 1362607**.** **https://doi.org/10.3389/fnins.2024.1362607**

34. Tanji, J. (1994). The supplementary motor area in the cerebral cortex. *Neuroscience Research*, 19(3), 251–268. **https://doi.org/10.1016/0168-0102(94)90038-8[1**]

35. Tanji, J., & Kurata, K. (1982). Comparison of movement-related activity in two cortical motor areas of primates. *Journal of Neurophysiology*, 48(3), 633–653. **https://doi.org/10.1152/jn.1982.48.3.633**

36. Tanji, J., & Kurata, K. (1985). Contrasting neuronal activity in supplementary and precentral motor cortex of monkeys. I. Responses to instructions determining motor responses to forthcoming signals of different modalities. *Journal of Neurophysiology*, 53(1), 129–141. **https://doi.org/10.1152/jn.1985.53.1.129**

37. Crammond, D. J., & Kalaska, J. F. (2000). Prior information in motor and premotor cortex: Activity during the delay period and effect on pre-movement activity. *Journal of Neurophysiology*, 84(2), 986–1005. **https://doi.org/10.1152/jn.2000.84.2.986**